J.G., manuscript submitted). HeLa whole-cell extract (200 mg) in CHB buffer (10 mM HEPES, pH 7.9, 0.2 mM EDTA, 0.2 mM EGTA, 5 mM β-glycerophosphate, 1 mM DTT, 50 μM $ZnCl_2$, 0.05% N-P40, 12% glycerol) plus 50 mM NaCl was chromatographed on a 1-ml GST–TFIIS column (10 mg per ml ligand), washed with 15 ml CHB-50 mM NaCl, then eluted with CHB-325 mM NaCl. 2 ml of eluate was loaded onto a Sepharose CL-2B column (60 × 1.6 cm; flow rate 0.4 ml min^{-1}) equilibrated with CHB-100 mM NaCl plus 8% glycerol, and 4-ml fractions were collected.

Received 31 July; accepted 22 November 1996.

1. Yuryev, A. *et al. Proc. Natl Acad. Sci. USA* **93,** 6975–6980 (1996).
2. Mortillaro, M. J. *et al. Proc. Natl Acad. Sci. USA* **93,** 8253–8257 (1996).
3. Gerber, H. P. *et al. Nature* **374,** 660–662 (1995).
4. Zehring, W. A., Lee, J. M., Weeks, J. R., Jokerst, R. S. & Greenleaf, A. L. *Proc. Natl Acad. Sci. USA* **85,** 3698–3702 (1988).
5. Nesic, D., Cheng, J. & Maquat, L. E. *Mol. Cell. Biol.* **13,** 3359–3369 (1993).
6. Niwa, M., Rose, S. D. & Berget, S. M. *Genes Dev.* **4,** 1552–1559 (1990).
7. Connelly, S. & Manley, J. L. *Genes Dev.* **2,** 440–452 (1988).
8. Logan, J., Falck, P. E., Darnell, J. E. J. & Shenk, T. *Proc. Natl Acad. Sci. USA* **84,** 8306–8310 (1987).
9. Whitelaw, E. & Proudfoot, N. *EMBO J.* **5,** 2915–2922 (1986).
10. Usheva, A. *et al. Cell* **69,** 871–881 (1992).
11. Takagaki, Y. & Manley, J. L. *J. Biol. Chem.* **267,** 23471–23474 (1992).
12. Ossipow, V., Tassan, J. P., Nigg, E. A. & Schibler, U. *Cell* **83,** 137–146 (1995).
13. Maldonado, E. *et al. Nature* **381,** 86–89 (1996).
14. Smale, S. T. & Tijan, R. *Mol. Cell. Biol.* **5,** 5352–5362 (1985).
15. Sisodia, S. S., Sollner, W. B. & Cleveland, D. W. *Mol. Cell. Biol.* **7,** 3602–3612 (1987).
16. Mifflin, R. C. & Kellems, R. E. *J. Biol. Chem.* **266,** 19593–19598 (1991).
17. Greenleaf, A. L. *Trends Biochem. Sci.* **18,** 117–119 (1993).
18. Beyer, A. L. & Osheim, Y. N. *Genes Dev.* **2,** 754–765 (1988).
19. Wuarin, J. & Schibler, U. *Mol. Cell Biol.* **14,** 7219–7225 (1994).
20. Lutz, C. S. *et al. Genes Dev.* **10,** 325–337 (1996).
21. Boelens, W. C. *et al. Cell.* **72,** 881-892 (1993).
22. Zhang, G., Taneja, K. L., Singer, R. H. & Green, M. R. *Nature* **372,** 809–812 (1994).
23. Mattaj, I. W. *Nature* **372,** 727–728 (1994).
24. Schul, W. *et al. EMBO J.* **15,** 2883–2892 (1996).
25. Blau, J. *et al. Mol. Cell. Biol.* **16,** 2044–2055 (1996).
26. Lieber, A., Kiessing, U. & Strauss, M. *Nucleic Acids Res.* **17,** 8485–8493 (1989).
27. West, M. & Corden, J. *Genetics* **140,** 1223–1233 (1995).
28. Peterson, S. R., Dvir, A., Anderson, C. W. & Dynan, W. S. *Genes Dev.* **6,** 426–438 (1992).
29. Dignam, J. D., Lebovitz, R. M. & Roeder, R. G. *Nucleic Acids Res.* **11,** 1475–1489 (1983).
30. Jenny, A., Minvielle-Bastia, L., Preker, P. & Keller, W. *Science* **274,** 1514–1517 (1996).

Acknowledgements: S.McC., N.F. and K.Y. contributed equally to this work. We thank J. Blau, P. Atadja and B. McNeil for their contribution; J. Corden, M. West and A. Yuryev for plasmids and for sharing unpublished data; R. Treisman and L. Harrington for discussion. J. Manley, W. Keller, A. Jenny, P. O'Hare, E. Lees, J.-M. Egly, M. Rihanek, T. Zamborelli, M. Pandes, J. Biron, S. Suggs and the Amgen EST Program for antibodies, HeLa cells and CstF plasmids; and A. Hessel, H. Agah, M. Pandes, P. Courchesne, B. Bolychuk and S. Pang for computer, technical, photographic and secretarial assistance.

Correspondence and requests for materials to D.B. (e-mail: david.bentley@amgen.com).

Structure of the conserved GTPase domain of the signal recognition particle

Douglas M. Freymann, Robert J. Keenan, Robert M. Stroud & Peter Walter

Department of Biochemistry and Biophysics, School of Medicine, University of California, San Francisco, California 94143-0448, USA

The signal-recognition particle (SRP) and its receptor (SR) function in the co-translational targeting of nascent protein–ribosome complexes to the membrane translocation apparatus[1]. The SRP protein subunit (termed Ffh in bacteria) that recognizes the signal sequence of nascent polypeptides is a GTPase, as is the SR-α subunit (termed FtsY)[2,3]. Ffh and FtsY interact directly, each stimulating the GTP hydrolysis activity of the other[4]. The sequence of Ffh suggests three domains: an amino-terminal N domain of unknown function, a central GTPase G domain, and a methionine-rich M domain that binds both SRP RNA and signal peptides[5,6]. Sequence conservation suggests that structurally similar N and G domains are present in FtsY[7,8]. Here we report the structure of the nucleotide-free form of the NG fragment of Ffh. Consistent with a role for apo Ffh in protein targeting, the side chains of the empty active-site pocket form a tight network of interactions which may stabilize the nucleotide-free protein. The structural relationship between the two domains suggests that the N domain senses or controls the nucleotide occupancy of the GTPase domain. A structural subdomain unique to these evolutionarily conserved GTPases constitutes them as a distinct subfamily in the GTPase superfamily[9].

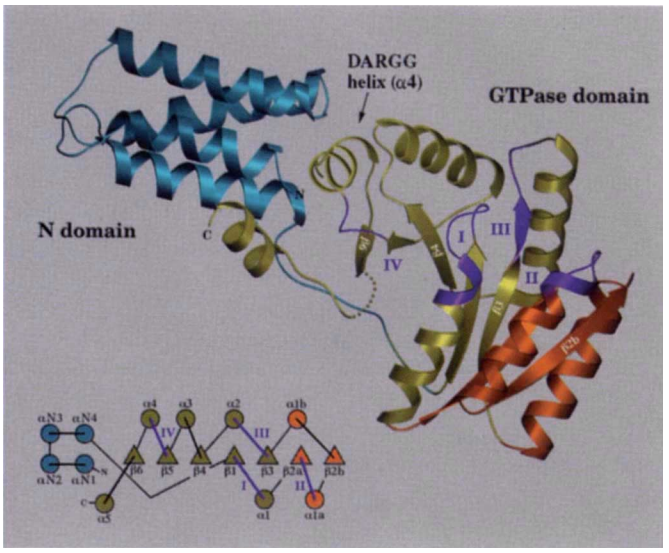

Figure 1 Structure and topology of the NG domain. The four-helix bundle of the N domain (blue) is closely associated with the GTPase domain (green and orange). The loops containing the conserved GTPase sequence motifs I (105–112), II (135–141), III (187–192), and IV (245–248) are highlighted (purple); these define the position of the GTP-binding site. The interface between the two domains occurs primarily along a single, distorted helix (the 'DARGG' helix). The main structural difference distinguishing the GTPase of Ffh from other GTPases is the subdomain, coloured orange, inserted between helix α1 and strand β3 of the core GTPase fold. The α-helices and β-strands are numbered in accordance with their structural counterparts in $p21^{ras}$. An eight-residue loop cannot be seen in the electron-density map and is probably disordered because of the absence of bound nucleotide; it is indicated by the dotted line.

The structure of the apo form of Ffh NG (Fig. 1) was determined to a resolution of 2.05 Å by X-ray diffraction using multiple isomorphous replacement (Table 1). The G domain has a β/α fold that is structurally similar to other GTPases in the superfamily including $p21^{ras}$ (Ras)[10], EF-G[11,12] and transducin Gα[13]. The N domain is a bundle of four antiparallel α-helices, which open at one end, allowing sidechains of the G domain to complete the packing of its hydrophobic core. The protein is thus a single structural unit in which the two sequence domains, N and G, are distinct, yet closely associated. A ten-residue peptide that links the two domains is packed tightly against the protein surface, rendering the NG fragment stable to proteolysis[5,14].

The core GTPase fold is a five-stranded β-sheet surrounded by α-helices; loops between the β-strands of the sheet and the α-helices contain four highly conserved sequence motifs (I–IV) which mediate interaction with the bound ribonucleotide[15] (Fig. 1, purple). Two striking structural differences distinguish the G domain of Ffh from other subfamilies of GTPases. The first is the subdomain (Fig. 1, orange), which includes motif II (G–2)[15]; this region is highly conserved within, but not between, subfamilies of GTPases, and in Ras and other GTPases it is known to interact with GTPase-activating proteins[9]. As Ffh and FtsY mutually stimulate GTP hydrolysis[4], the subdomain is likely to function in the interaction between the Ffh and its receptor. It is an insertion of 50 amino acids that extends the core β-sheet by two strands and two helices to form a seven-stranded all-parallel β-sheet. The first

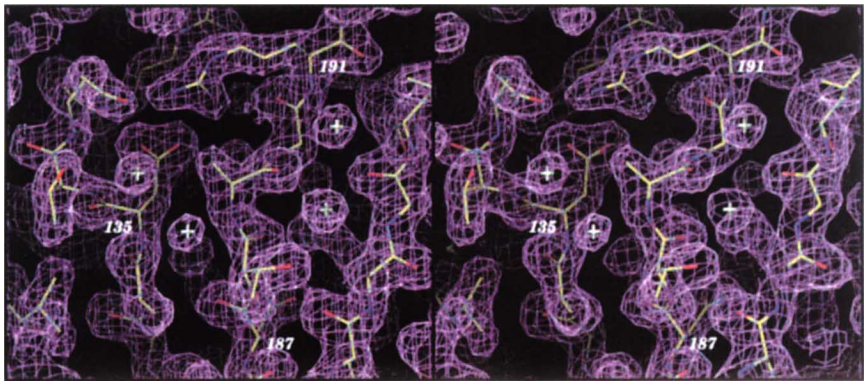

Figure 2 Stereo view of the 2.05-Å resolution electron-density map contoured at 1.25 σ obtained after phase combination with the experimental MIR phases. The positions of several water molecules are marked (+). The side chains of Asp 135 and Arg 191 form a salt bridge. These residues are part of conserved GTPase motifs II and III, respectively, and Arg 191 is proposed to interact with the bound GTP; if so, the side chains must rearrange during the GTPase cycle of Ffh.

connecting loop of the subdomain, between β2a and α1a (Fig. 1, insert), contains the conserved motif II, which forms part of the predicted nucleotide-binding pocket. The second striking difference between the G domain and other GTPases occurs at the C-terminal helix. In all other GTPases for which a structure is known, a C-terminal helix packs against the first helix (α1) of the fold. In the G domain of NG, there is no corresponding helix; the space is filled primarily by the side chains from the extended N–G linker peptide. Instead, a helix is splayed out, away from the G domain, so that its C terminus is packed against a face of the N-domain helical bundle.

We can propose roles for several of the conserved residues in the G-domain active site by analogy to the structures of other GTPases complexed with bound nucleotide[16–18]; thus Lys 111 of conserved sequence motif I interacts with the β-phosphate; Arg 138 of motif II stabilizes the γ-phosphate leaving group; Asp 187 of motif III ligates Mg^{2+}, and Arg 191 of motif III stabilizes the nucleophilic water molecule. At the other end of the G domain, Asp 248 of motif IV provides specificity for the guanine base; that this is its function in the G domain of FtsY has been shown by mutation to Asn to yield an XTP-specific activity[4]. In contrast to these proposed functional roles in interaction with bound Mg^{2+}-GTP, it is striking that, in the structure of the apo form of the NG fragment, the side chains of motifs I, II and III form instead a tight network of interactions among themselves (Figs 2 and 3). Thus the active-site side chains in the apo form of the G domain are effectively sequestered, and a substantial structural rearrangement must accompany the formation of the catalytically competent complex with Mg^{2+}-GTP. Such structural changes may either allow interaction with, or may be made more favourable by interaction with, FtsY or other ligands. In the structures of apo EF-G and magnesium-free EF-G/GDP complex, the corresponding conserved lysine and aspartate residues are in a conformation similar to that seen here[19]. Other GTPases are generally unstable in the absence of bound nucleotide. The network of interactions seen here may therefore provide a mechanism for stabilization of the empty state[20].

GTPases cycle between an 'activated' GTP-bound state and an 'inactive' GDP-bound state[9,15]. Relatively small local conformational changes that accompany this 'phosphate switch' are amplified by

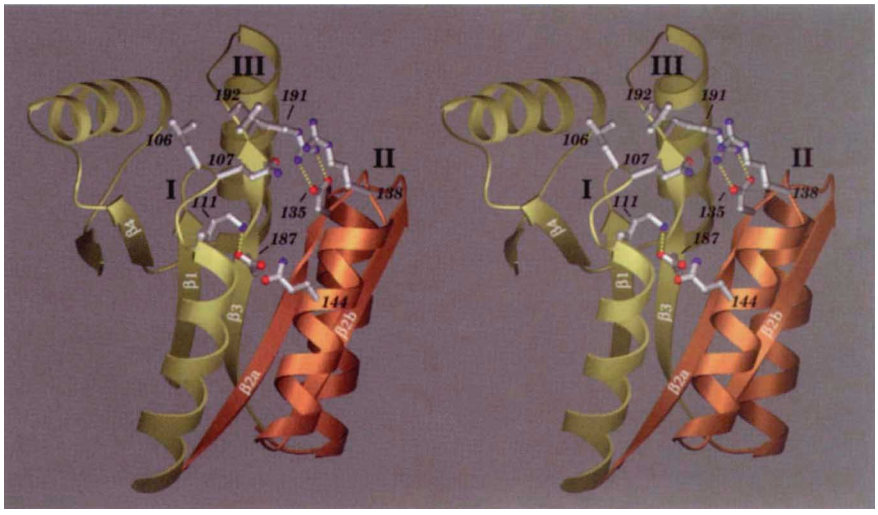

Figure 3 Highly conserved side chains of GTPase motifs I, II and III in the active site of Ffh. In other GTPase structures these side chains interact with the bound ribonucleotide and with the Mg^{2+} required for catalysis, and stabilize the transition state during hydrolysis of the bound GTP[16–18]. In the apo form of the Ffh NG fragment they form a tight network of interactions. Two in particular are noted: Lys 111, of conserved motif I, forms a salt bridge with Asp 187 of motif III. The Asp in this position has a role in ligating the Mg^{2+} in other GTPase structures[19]. Arg 191, also part of motif III, is in the structural position, corresponding to Gln 61 of Ras and Gln 200 of transducin Gα, which functions to stabilize the attacking water molecule in the transition state[16,21]. Here it is sequestered by formation of a salt bridge with Asp 135 of conserved motif II. Gln 144 reaches towards the motif I loop and presumably can interact with the α- and β-phosphate oxygens of bound nucleotide. The hydrophobic residues Leu 106 and Leu 192 are exposed to solvent near the active site. Accessible hydrophobic side chains often contribute to protein interaction surfaces (as they do in EF-Tu[17]); here they may define part of the region of the NG surface recognized by FtsY or by the C-terminal M domain of Ffh.

Table 1 Crystallographic statistics

Data collection

Data set	Resolution (Å)	R_{sym} (%)*	Redundancy†	Completeness (%)‡
Native	2.05	4.6 (13.7)	4.0 (3.9)	99 (98)
K_3IrCl_6	2.80	4.1 (5.9)	3.2 (3.1)	99 (98)
$Pt(NH_3)_2$	2.60	5.2 (8.0)	3.3 (3.2)	97 (91)
$PtCl_4$	2.80	5.8 (15.7)	3.6 (3.4)	97 (95)
K_2HgI_4	2.80	4.7 (6.9)	3.8 (3.8)	97 (96)

MIR phasing

Derivative	R_{der} (%)§	Resolution cutoff (Å)	Sites	Phasing power‖	$R_{centric}$ (%)¶
K_3IrCl_6	20 (24)	2.8	1	1.82 (1.37)	54 (68)
$Pt(NH_3)_2$	22 (21)	3.5	4	1.45 (0.83)	61 (80)
$PtCl_4$	15 (22)	3.5	2	1.22 (0.72)	73 (88)
K_2HgI_4	16 (18)	4.8	4	2.62 (1.34)	42 (78)

Overall figure of merit to 3.5 Å = 0.64

Refinement

	R_{cryst}# (%)	R_{free} (%)	Resolution (Å)	Reflections #	Protein atoms	Water atoms
$F > \sigma(F)$	20.2	26.9	20.0–2.05	16,157	2,228	104

Values in parentheses are the high resolution bin.
*$R_{sym} = \Sigma|I_h - \langle I_h\rangle|/\Sigma I_h$, where $\langle I_h\rangle$ is the average intensity over symmetry equivalents.
† Redundancy is the average number of observations of each unique reflection.
‡ Completeness is the fraction of theoretically possible reflections observed at least once.
§$R_{der} = \Sigma|F_{ph} - F_p|/\Sigma F_p$, or mean fractional isomorphous difference.
‖ Phasing power $\langle f_h\rangle/\langle E\rangle$, where $\langle f_h\rangle$ is the r.m.s. of the heavy-atom structure-factor amplitude, and $\langle E\rangle$ is the r.m.s. lack of closure error.
¶$R_{centric} = \Sigma||F_{ph} \pm F_p| - f_h|/\Sigma|F_{ph} \pm F_p|$ for centric reflections.
#$R_{cryst} = \Sigma|F_o - F_c|/\Sigma F_o$. R_{free} was calculated for a subset of reflections (10%) omitted from the refinement.

intra- and intermolecular interactions[17,21,22], which centre around the phosphate-binding pocket. The structure of the NG fragment reveals, however, that the N and G domains interact along a distinct face of the G domain distant from the phosphate-binding pocket (Fig. 4). Extensive hydrophobic and electrostatic interactions between the domains are localized to the α4 helix, or 'DARGG' helix, of the G domain and the loop preceding it (Fig. 5), and follow immediately the conserved motif IV (Thr 245 to Asp 248), which mediates interaction with the guanine base. The amino-acid sequence in the interface is highly conserved in all members of the Ffh/FtsY family. In particular, a basic residue corresponding to Arg 252 and an acidic residue corresponding to Asp 42 are almost universally conserved, as are the residues at the positions of Gly 253 and Leu 257. The conservation of this interaction implies a role for this structure in the function of Ffh and its receptor, and suggests that the N domain is responsive to features distinct from the classic 'phosphate switch'. Its close proximity to motif IV, which interacts with the guanine base, suggests that the DARGG interaction is involved in sensing or controlling the nucleotide occupancy of the G domain.

The N and G domains are a structural and functional unit that is conserved between Ffh and its receptor, both proteins functioning along the pathway which targets nascent polypeptides to the membrane. The interaction between Ffh and its receptor, FtsY, both in the GTP-bound form, which causes stimulation of one GTPase by the other, is likely to involve the motif II subdomain, which forms part of the GTPase active site. We can imagine that these regions in Ffh and FtsY, which should exhibit conformational changes upon binding GTP, interact directly. Alternatively, the two proteins might interact in a head-to-tail fashion, with the N domain of one interacting with and stimulating the activity of the G domain of the other. We speculate that, as a consequence of these interactions and the concomitant conformational changes, the affinity of signal sequence binding to the M domain of Ffh is regulated to allow loading and unloading of the nascent chain at defined steps in the targeting cycle. □

Methods

Ffh was cloned from *Thermus aquaticus* and expressed and purified as described (D.M.F. *et al.*, manuscript in preparation). The NG fragment was generated by

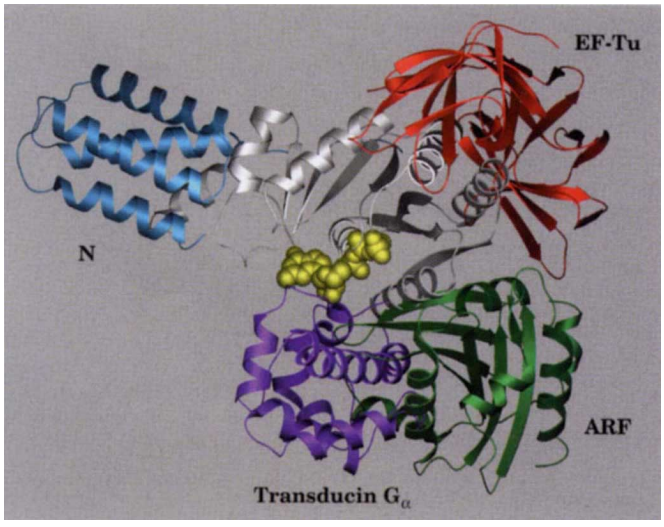

Figure 4 The relative positions, in four different GTPases, of the domains which interact with the GTPase domain of each protein. Shown are the N domain of Ffh; domains II and III of EF-Tu; the dimer interaction of ARF; and the helical insertion domain of transducin Gα. Here, the top of the GTPase domain in Fig. 1 has been rotated 90° towards the viewer. The predicted position of bound nucleotide triphosphate is indicated by the yellow space-filling model. The interactions of most known GTPases are localized to the phosphate switch' side of the GTPase fold and seem to function by sensing the 'activated', or GTP-bound, state of the protein which causes structural change in that region. In contrast, the N domain interacts at the opposite end of the G domain, suggesting a mechanism that senses or controls nucleotide occupancy distinct from other GTPases.

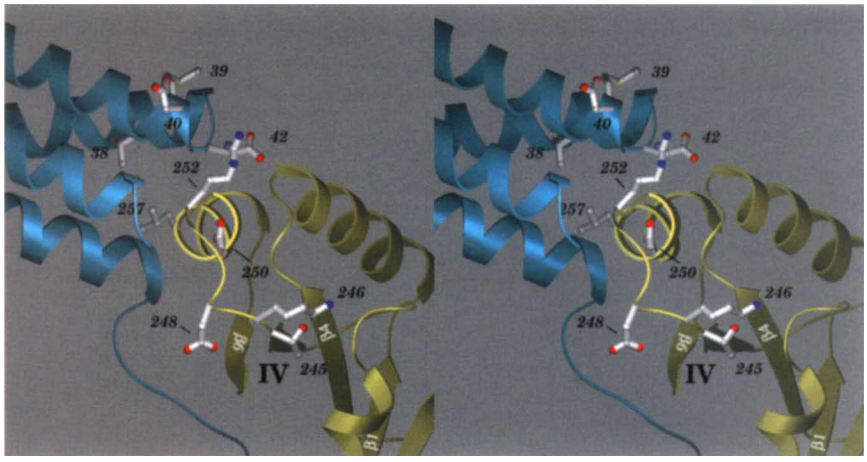

Figure 5 Details of the interface between the N and GTPase domains of Ffh. Highly conserved side chains of GTPase motif IV (residues 245–248), helix α4 (residues 250–257), and the N domain between helices αN2 and αN3 (residues 38–42) are shown; the C-terminal helix of the G domain is omitted for clarity. In prokaryotes, the sequence of residues 250–254, DARGG, is almost universally conserved. Asp 250 functions to initiate the helix through water-mediated interaction with the helix dipole; Arg 252 of the DARGG motif reaches across between the side chains of Asp 40 and Asp 42 of the N domain; Gly 253, with $\phi = 104°$, $\psi = 5°$, and Gly 254 allow the close approach of the N and G domains. Leu 257, also highly conserved, inserts into the open end of the N-domain helical bundle and completes that domain's hydrophobic core. The region of the N domain which contributes to this contact is the most highly conserved in the sequence of that domain.

proteolysis, in which protein at 1 mg ml^{-1} in 50 mM Pipes, pH 7.0, 2 mM $MgCl_2$, 250 mM NaCl was digested using 0.01 mg ml^{-1} elastase for 1 h, the reaction stopped with 100 mM AEBSF, and the product purified by anion-exchange high-performance liquid chromatography (HPLC). The protein was then concentrated to 30 mg ml^{-1} in water using a Centricon, and crystallization performed in sitting drops over a solution of 30% PEG monomethylether 550, 100 mM TAPS, pH 9.0, 200 mM $MgCl_2$ at room temperature. The crystals grew in space group $C2$, with $a = 99.9$ Å, $b = 53.9$ Å, $c = 57.4$ Å, $\beta = 119.8°$. As the crystals formed in a cryoprotectant mother liquor, they could be frozen easily, and each dataset was collected from a single crystal in a stream of nitrogen at −170 °C. Native and heavy-atom derivative data were collected using MAR30 and RAXIS II image plate detectors mounted on a Rigaku X-ray source. Data were processed using DENZO and SCALEPACK[23] with no sigma cutoff. Subsequent data processing was with the CCP4 package[24]. Four heavy-atom soak conditions yielded useful derivatives; only one, K_3IrCl_6, contributed to phasing beyond 3.5 Å resolution. Heavy-atom parameters were refined using MLPHARE[24]. The resolution limit applied to each derivative dataset during phase calculation was determined by inspection of difference Patterson maps and the behaviour of the statistical indicators fh/E and $R_{centric}$ on resolution. The initial MIR electron-density map was calculated at 3.5 Å resolution. This map clearly revealed the position of the β-sheet that was expected to form the core of the GTPase fold. An iterative process of building, refinement and phase combination[25] yielded a poly-Ala model which accounted for nearly all of the observed main-chain density (although without sequence or correct connectivity). It was refined, in one step, against the full data set and used to calculate a map to 2.05 Å resolution. This map enabled us to build the complete amino-acid sequence. The atomic model was built using O[26], and the structure was refined using X-PLOR[27]. Data to a low resolution limit of 20.0 Å were included in the refinement after applying a bulk solvent correction. A subset (10%) of the data were set aside for calculation of R_{free}[27] before any crystallographic refinement (including that of the poly-Ala model) was done. The electron-density map is extremely clear, and the polypeptide is generally in well-defined electron density (Fig. 2). The current model extends from Phe 2 to Gly 297; another two or three disordered C-terminal residues may be present. The loop from Gly 271 to Gly 278 cannot be seen in the electron-density map and is presumably disordered. Arg 128 is modelled with two conformations. No Mg^{2+} ions have been located in the structure. The crystals of NG diffract to 1.0 Å resolution; a complete analysis of the structure using data to that resolution, including the water structure and the determinants of thermostability, will be presented elsewhere. For comparison with the structures of other GTPases, the G domains of EF-Tu (left)[28], ARF (1hur)[29] and transducin Gα (1tnd)[13] were superimposed on the G domain of Ffh using the motif I loop and β-strands β1, β4 and β5 of the core GTPase fold. The positions of the domains in intra- and intermolecular contact with the GTPase domain are shown in Fig. 4. The structure of EF-G,which was omitted from the figure for clarity, has a G′ subdomain that occurs near, but does not overlap with, the position of the N domain in Ffh. Figures were generated using O[26] and SETOR[30].

Received 27 September; accepted 22 November 1996.

1. Walter, P. & Johnson, A. E. *Annu. Rev. Cell Biol.* **10,** 87–119 (1994).
2. Miller, J. D., Bernstein, H. D. & Walter, P. *Nature* **367,** 657–659 (1994).
3. Kusters, R. *et al. FEBS Lett.* **372,** 253–258 (1995).
4. Powers, T. & Walter, P. *Science* **269,** 1422–1424 (1995).
5. Zopf, D., Bernstein, H. D. & Walter, P. *J. Cell Biol.* **120,** 1113–1121 (1993).
6. Römisch, K., Webb, J., Lingelbach, K., Gausepohl, H. & Dobberstein, B. *J. Cell Biol.* **111,** 1793–1802 (1990).
7. Bernstein, H. D. *et al. Nature* **340,** 482–486 (1989).
8. Römisch, K. *et al. Nature* **340,** 478–482 (1989).
9. Bourne, H. R., Sanders, D. A. & McCormick, F. *Nature* **348,** 125–132 (1990).
10. Pai, E. F. *et al. Nature* **341,** 209–214 (1989).
11. Czworkowski, J., Wang, J., Steitz, T. A. & Moore, P. B. *EMBO J.* **13,** 3661–3668 (1994).
12. Ævarsson, A. *et al. EMBO J.* **13,** 3669–3677 (1994).
13. Noel, J. P., Hamm, H. E. & Sigler, P. B. *Nature* **366,** 654–663 (1993).
14. Lütcke, H., High, S., Römisch, K., Ashford, A. J. & Dobberstein, B. *EMBO J.* **11,** 1543–1551 (1992).
15. Bourne, H. R., Sanders, D. A. & McCormick, F. *Nature* **349,** 117–127 (1991).
16. Sondek, J., Lambright, D. G., Noel, J. P., Hamm, H. E. & Sigler, P. B. *Nature* **372,** 276–279 (1994).
17. Berchtold, H. *et al. Nature* **365,** 126–132 (1993).
18. Prive, G. G. *et al. Proc. Natl Acad. Sci. USA* **89,** 3649–3653 (1992).
19. Al-Karadaghi, S., Ævarsson, A., Garber, M., Zheltonosova, J. & Liljas, A. *Structure* **4,** 555–565 (1996).
20. Miller, J. D., Wilhelm, H., Gierasch, L., Gilmore, R. & Walter, P. *Nature* **366,** 351–354 (1993).
21. Milburn, M. V. *et al. Science* **247,** 939–945 (1990).
22. Lambright, D. G. *et al. Nature* **379,** 311–319 (1996).
23. Otwinowski, Z. in *Data Collection and Processing* (eds Sawyer, L., Isaacs, N. W. & Bailey, S.) 55–62 (SERC Daresbury Laboratory, Warrington, 1993).
24. Collaborative Computational Project Number 4. *Acta Crystallogr. D* **50,** 760–763 (1994).
25. Read, R. J. *Acta Crystallogr. A* **42,** 140–149 (1986).
26. Jones, T. A., Zou, J. Y., Cowan, S. W. & Kjeldgaard, M. *Acta Crystallogr. A* **47,** 110–119 (1991).
27. Brünger, A. T. *X-PLOR: A System for X-Ray Crystallography and NMR* (Yale Univ. Press, New Haven, 1992).
28. Kjeldgaard, M., Nissen, P., Thirup, S. & Nyborg, J. *Structure* **1,** 35–50 (1993).
29. Amor, J. C., Harrison, D. H., Kahn, R. A. & Ringe, D. *Nature* **372,** 704–708 (1994).
30. Evans, S. V. *J. Mol. Graph.* **11,** 134–138 (1993).

Acknowledgements: We thank P. Peluso and T. Powers for discussions; P. Focia for assistance with data collection; and H. Bourne for encouragement and comments on the manuscript. This work was supported by fellowships from the Herb Boyer Fund and the Biotechnology Program of the University of California (D.M.F.) and by grants from the NIH (R.M.S. and P.W.).

Correspondence and requests for materials should be addressed to D.M.F. (e-mail: freymann @msg.ucsf.edu). Coordinates and structure factors have been deposited with the Protein Data Bank, accession no. 1ffh.